Journal of Alloys and Compounds 527 (2012) 226–232

Contents lists available at SciVerse ScienceDirect

Journal of Alloys and Compounds

journal homepage: www.elsevier.com/locate/jallcom

Effects of Zn addition and aging treatment on tensile properties of Sn–Ag–Cu alloys

Naoyuki Hamada [a,*], Tokuteru Uesugi [b], Yorinobu Takigawa [b], Kenji Higashi [b]

[a] Ishikawa Metal Co., Ltd., Sakai 592-8352, Japan
[b] Department of Materials Science, Graduate School of Engineering, Osaka Prefecture University, Sakai 599-8531, Japan

ARTICLE INFO

Article history:
Received 17 October 2011
Received in revised form 28 February 2012
Accepted 2 March 2012
Available online xxx

Keywords:
Pb-free solder
Microstructure
Scanning electron microscopy
X-ray diffraction

ABSTRACT

The effects of adding small amounts of Zn and conducting an aging treatment at elevated temperatures on the microstructure and tensile properties of low-Ag Sn–Ag–Cu alloys were investigated. The addition of Zn to Sn–Ag–Cu alloys inhibited the growth of intermetallic compounds. As the amount of Zn increased, the flow stress increased both before and after the aging treatment. In particular, the Sn–1Ag–0.3Cu–1Zn alloy exhibited the highest flow stress among all the examined alloys. Although the flow stress of the Sn–3Ag–0.5Cu alloy was originally higher than that of the Sn–1Ag–0.1Cu–0.4Zn and Sn–1Ag–0.3Cu–0.7Zn alloys, the flow stress of these two alloys was higher after aging for 500 h at 398 K than that of the Sn–3Ag–0.5Cu alloy. The addition of small amounts of Zn in Sn–Ag–Cu alloys suppressed the decline in the flow stress after the aging treatment.

1. Introduction

Eutectic Sn–37Pb solder has been the most widely used material for interconnecting and packaging electronic components. However, Pb and Pb-containing compounds are considered toxic. Owing to environmental concerns and health hazards associated with Pb, several studies have focused on Pb-free solders and soldering techniques aiming at replacing Sn–Pb solders with Pb-free alternatives [1–4].

Several Pb-free solder alloys have been developed, including Sn–Zn, Sn–Ag, Sn–Cu, Sn–Bi, and Sn–Ag–Cu alloys. The near-ternary eutectic Sn–Ag–Cu alloys are regarded as one of the most attractive among them because of their excellent wettability and mechanical properties [5–7]. Near-ternary eutectic Sn–Ag–Cu alloys such as Sn–3Ag–0.5Cu or Sn–3.8Ag–0.7Cu are the most well-known Pb-free solders worldwide [7,8]. The wettability properties and interfacial reactions in the near-eutectic Sn–Ag–Cu alloys during soldering have been studied recently [9–15]. However, these alloys contain approximately 3 wt.% of Ag (an expensive metal), which makes them more expensive than other Pb-free solders. Sn–Ag–Cu alloys with lower Ag content, referred to as low-Ag Pb-free solders, such as Sn–1Ag–0.5Cu and Sn–0.3Ag–0.7Cu, have been developed recently in order to reduce the material cost [16,17]. However, the decrease in the Ag content reduces the mechanical strength (e.g., ultimate strength, creep resistance, flow stress) [16,18–20]. Consequently, recent research has focused on finding a fourth element to boost the mechanical strength of low-Ag Sn–Ag–Cu solders [21,22].

In a previous study, we investigated Sn–Zn alloys and showed that the addition of small amounts of Zn, up to ~0.4 wt.%, can significantly improve the creep resistance owing to solid solution strengthening [23]. Small amounts of Zn are expected to improve the mechanical strength of low-Ag Sn–Ag–Cu alloys. The addition of small amounts of Zn to near-ternary eutectic Sn–Ag–Cu solders is also reported to limit the formation of large Ag_3Sn intermetallic compounds and improve the mechanical strength of solder alloys [24–26]. Moreover, the addition of small amounts of Zn to Sn–Ag–Cu solders has received considerable attention because it can slow the growth of intermetallic compounds and inhibit the formation of Kirkendall voids and the growth of whiskers on the surface [27–36]. Song et al. reported very recently that the mechanical strength of Sn–1Ag–0.5Cu was increased by the addition of up to 1 wt.% of Zn [21]. However, no studies have yet investigated the thermal stability of low-Ag Sn–Ag–Cu–Zn alloys in terms of their mechanical strength.

Solder alloys are used to form joints between electronic components and printed circuit boards. The strength of solder joints is affected by the thermal stability of the solder alloys. Solder joints must exhibit long-term reliability under extreme conditions, particularly at high temperatures. Because the mechanical strength of Pb-free solders is critical to their reliability, it is important to understand the effect of high-temperature aging on the mechanical strength of Pb-free solder alloys. It is well known that the mechanical strength of Sn–Ag–Cu solder joints is reduced after aging at

* Corresponding author at: 7-21 Chikko Hamadera Nishimachi, Sakai-city, Osaka 592-8352, Japan. Tel.: +81 72 268 1155; fax: +81 72 268 1159.
E-mail address: naoyuki_hamada@ishikawa-metal.com (N. Hamada).

0925-8388/$ – see front matter © 2012 Elsevier B.V. All rights reserved.
doi:10.1016/j.jallcom.2012.03.008

Table 1
Chemical compositions of Sn–Ag–Cu–Zn and Sn–Ag–Cu alloys (wt.%).

	Sn	Ag	Cu	Zn	Sb	Bi	Pb	Fe	In
Sn–3Ag–0.5Cu	Balance	3.01	0.462	0.0003	0.001	0.001	0.002	0.004	0.001
Sn–1Ag–0.7Cu	Balance	1.01	0.705	0.0004	0.001	0.002	0.002	0.002	0.001
Sn–1Ag–0.1Cu–0.4Zn	Balance	1.03	0.110	0.41	0.001	0.003	0.002	0.001	0.001
Sn–1Ag–0.3Cu–0.7Zn	Balance	1.02	0.303	0.71	0.001	0.002	0.002	0.001	0.001
Sn–1Ag–0.3Cu–1Zn	Balance	1.03	0.305	0.98	0.002	0.002	0.001	0.001	0.001

elevated temperatures (e.g., 398 K) [37]. This observation is related to the microstructural evolution of the solder joints. The formation and growth of intermetallic compounds in solder alloys greatly affect the mechanical strength of the solder joints [8,38].

The objective of this study is to investigate the effect of adding small amounts of Zn on the flow stress of low-Ag Sn–Ag–Cu alloys after aging at elevated temperature. In addition, we try to explain the reasons for the change in flow stress and the thermal stability in terms of the mechanical strength of Sn–Ag–Cu–Zn alloys.

2. Experimental procedures

Sn–3Ag–0.5Cu, Sn–1Ag–0.7Cu, Sn–1Ag–0.1Cu–0.4Zn, Sn–1Ag–0.3Cu–0.7Zn, and Sn–1Ag–0.3Cu–1Zn alloys were used in this study. For the preparation of these alloys, high-purity Sn (99.98%, Yunnan Chengfeng Non-ferrous Metals Co., Ltd., China), Ag (99.99%, Korea Zinc Co., Ltd., Korea), Cu (99.99%, Mitsuwa Chemicals Co., Ltd., Japan), and Zn (99.9%, Mitsuwa Chemicals Co., Ltd., Japan) were used as starting materials. The chemical compositions of the prepared alloys are listed in Table 1. The alloys were initially produced by the ingot casting technique at a casting temperature of 603 K. The molten alloys were cast into an iron mold having an inner diameter and length of 30 and 140 mm, respectively. To dissolve Zn into the Sn matrix, the ingots were heat-treated at 423 K for 24 h in air and then quenched in water. Subsequently, the ingots were extruded into cylindrical bars 12 mm in diameter at 373 K. The cylindrical bars were machined as tensile test specimens with a gage length of 12 mm and diameter of 4 mm. Tensile tests were conducted using the constant strain rate method and performed twice in each condition (as-extruded or aged). The aged samples were heat-treated at 398 K for 250, 500, and 1000 h in air before testing. The as-extruded specimens were tested at a strain rate of 1×10^{-3} s^{-1} at 298 and 398 K. The aged samples were tested at a strain rate of 1×10^{-3} s^{-1} at 398 K.

Scanning electron microscopy (SEM, Shimadzu, SSX-550) was used to examine the changes in the microstructure of the as-extruded and aged samples. X-ray diffraction (XRD) analysis (Rigaku, Ultima IV) using CuKα radiation was conducted to identify the intermetallic compounds.

3. Results

3.1. Microstructures

Fig. 1(a), (c), (e), (g), and (i) shows SEM photographs of the microstructures of Sn–Ag–Cu and Sn–Ag–Cu–Zn alloys before the aging treatment. Fig. 1(b), (d), (f), (h), and (j) shows the SEM photographs of microstructures of these alloys after they are aged for 500 h at 398 K. The intermetallic compounds appear bright in these micrographs; in contrast, the β-Sn phases are darker. The area of the intermetallic compound particles was measured by image processing. The average aspect ratios (ratio of major axis to minor axis for a given particle) ranged from 1.7 to 2.3 in the Sn–Ag–Cu and Sn–Ag–Cu–Zn alloys. Although the particles were not completely spherical, the particle diameter was estimated assuming that they were spherical. Fig. 2 shows the distribution of the particle diameters and the average particle diameter of the alloys. After aging, the intermetallic compound particles in all the alloys coarsened; moreover, the average particle diameters ranged from 0.92 to 1.05 μm in the Sn–Ag–Cu–Zn alloys and from 1.40 to 1.49 μm in the Sn–Ag–Cu alloys. The addition of Zn to Sn–Ag–Cu alloys inhibits the growth of intermetallic compounds.

Fig. 3 shows the XRD patterns of the alloys before the aging treatment. The XRD patterns of the Sn–3Ag–0.5Cu and Sn–1Ag–0.7Cu alloys indicate the presence of Ag_3Sn and Cu_6Sn_5 compounds. In the Sn–Ag–Cu system, Ag and Cu dissolve with difficulty in the Sn matrix to form intermetallic compounds of Ag_3Sn and Cu_6Sn_5 [39,40]. The maximum solubility limits of Ag and Cu in Sn–Ag and Sn–Cu are 0.04 wt.% and 0.0063 wt.%, respectively [41]. Only the peaks associated with Ag_3Sn were observed in the Sn–1Ag–0.1Cu–0.4Zn and Sn–1Ag–0.3Cu–0.7Zn alloys. We identified intermetallic compounds Ag_3Sn and Cu_5Zn_8 in the XRD pattern of the Sn–1Ag–0.3Cu–1Zn alloy. Previous work has also shown the formation of Ag_3Sn and Cu_5Zn_8 compounds in Sn–1Ag–0.5Cu–1Zn [21].

3.2. Flow stress

Fig. 4 shows the flow stress at 298 and 398 K before the aging treatment. The flow stress was determined at a fixed true strain of 0.1 for each sample tested at the given temperature and strain rate. Fig. 4 also includes the value for Sn–0.4Zn, which was studied in our previous paper [23]. Fig. 4 indicates that the flow stress of Sn–Ag–Cu–Zn alloys increases with increasing Zn content at 298 and 398 K. The addition of Zn clearly enhances the flow stress of low-Ag Sn–Ag–Cu alloys. In particular, the Sn–1Ag–0.3Cu–1Zn alloy exhibited the highest flow stress among all the examined alloys at 298 and 398 K.

The flow stress variation at 398 K as a function of the aging time in Sn–Ag–Cu and Sn–Ag–Cu–Zn alloys is shown in Fig. 5. In the Sn–3Ag–0.5Cu and Sn–1Ag–0.7Cu alloys, the flow stress decreased significantly with increasing aging time. Although the flow stress of the Sn–3Ag–0.5Cu alloy is higher than those of the Sn–1Ag–0.1Cu–0.4Zn and Sn–1Ag–0.3Cu–0.7Zn alloys, the flow stress of the Sn–3Ag–0.5Cu alloy declines more rapidly with aging treatment than that of the Sn–Ag–Cu–Zn alloys. The flow stress of the Sn–3Ag–0.5Cu alloy is lower after aging for 500 h than those of the Sn–1Ag–0.1Cu–0.4Zn and Sn–1Ag–0.3Cu–0.7Zn alloys. Fig. 5 also includes the value for Sn–1Ag–0.7Cu–0.7Zn, which was presented in our patent [42]. A comparison of Sn–1Ag–0.7Cu with Sn–1Ag–0.7Cu–0.7Zn reveals that the addition of Zn also suppresses the decline in the flow stress when the Ag and Cu content is the same. The addition of a small amount of Zn obviously suppresses the decline in the flow stress of Sn–Ag–Cu alloys after aging treatment. Fig. 6 shows the variation in the total elongation at 398 K as a function of the aging time for Sn–Ag–Cu and Sn–Ag–Cu–Zn alloys. The effect of the aging treatment on the total elongation was insignificant.

4. Discussion

The results of this study show that the addition of small amounts of Zn to Sn–Ag–Cu increases the flow stress. Ag_3Sn and Cu_6Sn_5 particles in Sn–Ag–Cu alloys are known to contribute to dispersion hardening [43–45]. In Sn–Ag–Cu–Zn alloys, previous work showed that with the addition of Zn, the Cu_6Sn_5 phases were replaced by Cu_5Zn_8 phases; this work also showed that the Cu_5Zn_8 particles contribute to dispersion hardening [21]. In this study, we also confirmed the presence of Cu_5Zn_8 peaks in the XRD patterns of the Sn–1Ag–0.3Cu–1Zn alloys.

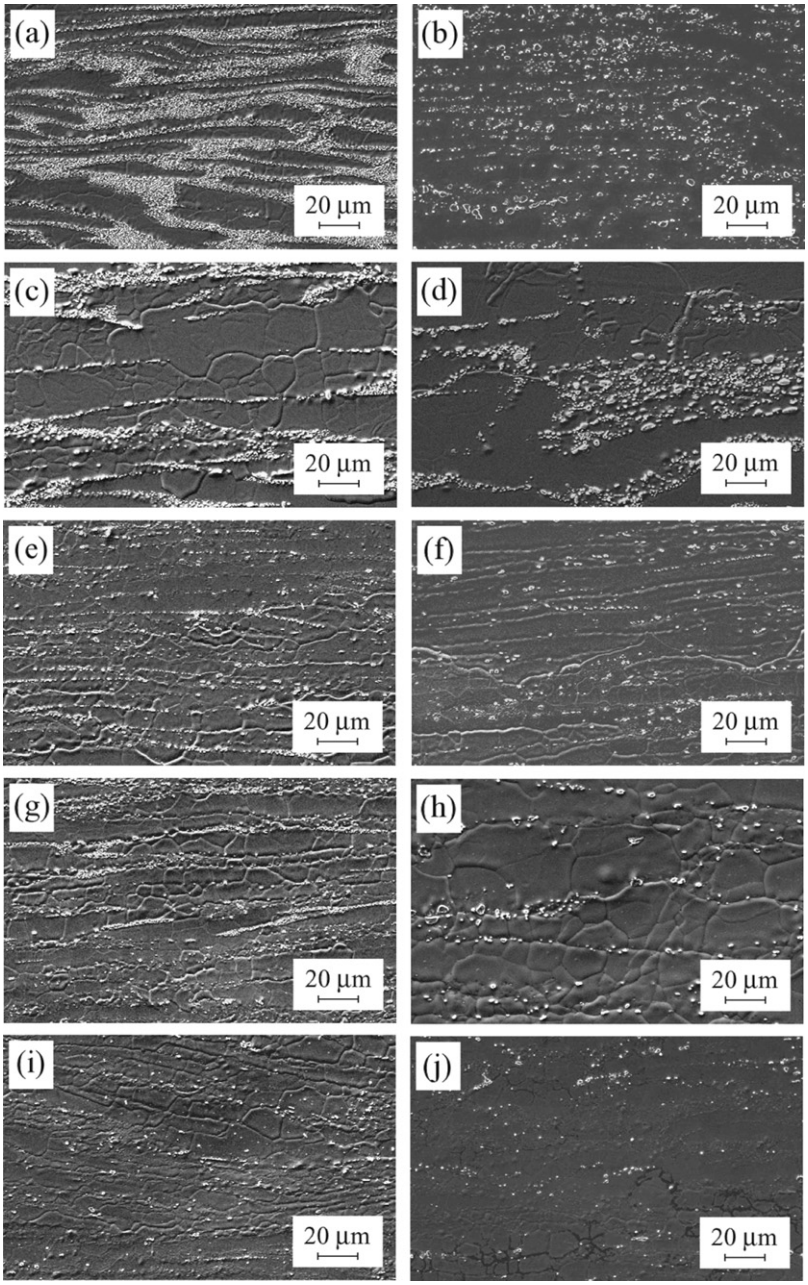

Fig. 1. SEM micrographs: (a), (c), (e), (g), and (i) show the microstructure of Sn–3Ag–0.5Cu, Sn–1Ag–0.7Cu, Sn–1Ag–0.1Cu–0.4Zn, Sn–1Ag–0.3Cu–0.7Zn, and Sn–1Ag–0.3Cu–1Zn, respectively, before aging; (b), (d), (f), (h), and (j) show the microstructure after aging at 398 K for 500 h.

Dispersion hardening is commonly attributed to the Orowan looping mechanism. The Orowan stress τ_{OR} can be estimated using the following equation [46]:

$$\tau_{OR} = \left(\frac{3}{2\pi}\right)\frac{\mu b}{r}f^{1/2}$$

where μ is the shear modulus (18.0 GPa [23]), b is Burger's vector (0.317 nm [47]), r is the average particle radius, and f is the volume fraction of intermetallic compounds. The average particle diameter is shown in Fig. 2. The Sn–Ag and Sn–Cu phase diagrams show negligible solid solubility of Ag and Cu in Sn [41]. Therefore, the volume fraction of intermetallic compounds was estimated assuming that all of the Ag and Cu form Ag_3Sn and Cu_6Sn_5 in Sn–Ag–Cu alloys. For Sn–Ag–Cu–Zn alloys, the volume fraction was estimated assuming that Cu preferentially forms Cu_5Zn_8 instead of Cu_6Sn_5. After Zn is preferentially consumed to form Cu_5Zn_8, the residual Zn is assumed to be in solution in the Sn matrix. On the basis of these assumptions, the Orowan stress before and after aging for 500 h at 398 K was determined (Table 2).

Before the aging treatment, the flow stress of the Sn–1Ag–0.3Cu–1Zn alloy was highest among those of all the Sn–Ag–Cu and Sn–Ag–Cu–Zn alloys, whereas its Orowan stress was smaller than that of the Sn–Ag–Cu alloys. The solubility

Table 2
Orowan stresses before and after aging for 500 h at 398 K.

	$\sigma_{OR}^{0\ h}$	$\sigma_{OR}^{500\ h}$	$\sigma_{OR}^{500\ h} - \sigma_{OR}^{0\ h}$
Sn–3Ag–0.5Cu	3.8	1.4	−2.4
Sn–1Ag–0.7Cu	2.0	1.0	−1.0
Sn–1Ag–0.1Cu–0.4Zn	1.3	1.1	−0.2
Sn–1Ag–0.3Cu–0.7Zn	1.7	1.3	−0.4
Sn–1Ag–0.3Cu–1Zn	1.7	1.5	−0.2

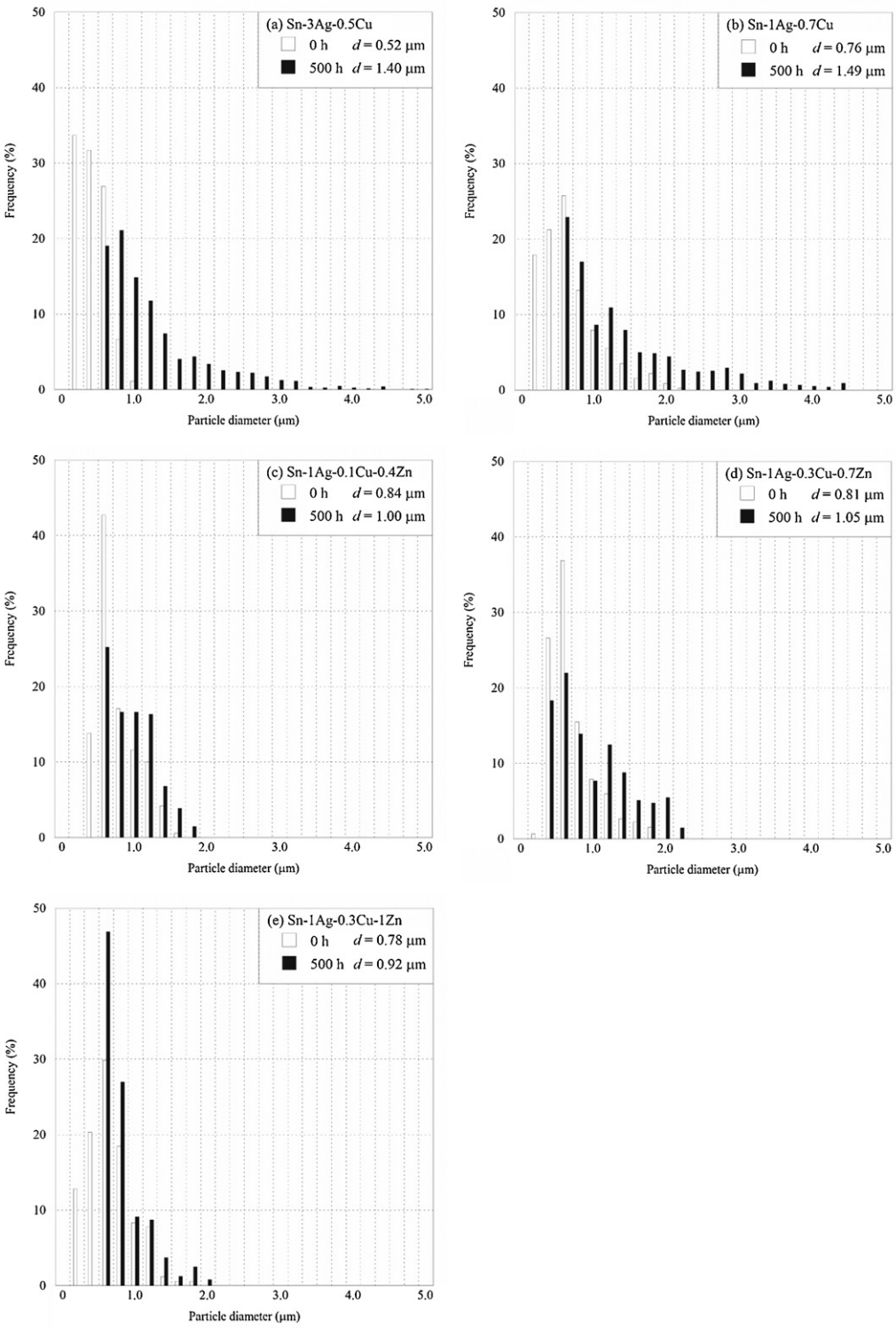

Fig. 2. Particle diameter distribution of the intermetallic compounds: (a)–(e) show the distributions before and after aging for 500 h at 398 K of Sn–3Ag–0.5Cu, Sn–1Ag–0.7Cu, Sn–1Ag–0.1Cu–0.4Zn, Sn–1Ag–0.3Cu–0.7Zn, and Sn–1Ag–0.3Cu–1Zn, respectively. The average diameter of the intermetallic compounds, *d*, is also shown in the legend box.

of Zn in Sn is very small, with a maximum solubility limit of 0.34 wt.% [48]. After Zn is preferentially consumed to form Cu_5Zn_8 in Sn–Ag–Cu–Zn alloys, part of the excess Zn remains in solution in the Sn matrix. In a previous work, we showed that the flow stress of Sn–Zn alloys was significantly improved by adding up to ~0.4 wt.% of Zn; the improvement was attributed to solid solution strengthening [23]. The flow stress of Sn–0.4Zn is also shown in Fig. 4. This flow stress, which was strengthened by solid solution hardening, is superior to that of Sn–1Ag–0.7Cu, which was strengthened by dispersion hardening. These results suggest that in addition to dispersion hardening, solid solution strengthening due to Zn contributes to the strengthening of Sn–Ag–Cu–Zn alloys.

The addition of small amounts of Zn to Sn–Ag–Cu suppressed the decline in the flow stress after the aging treatment. Here we describe how the Orowan looping mechanism explains dispersion hardening. The dispersed particles obstruct the motion

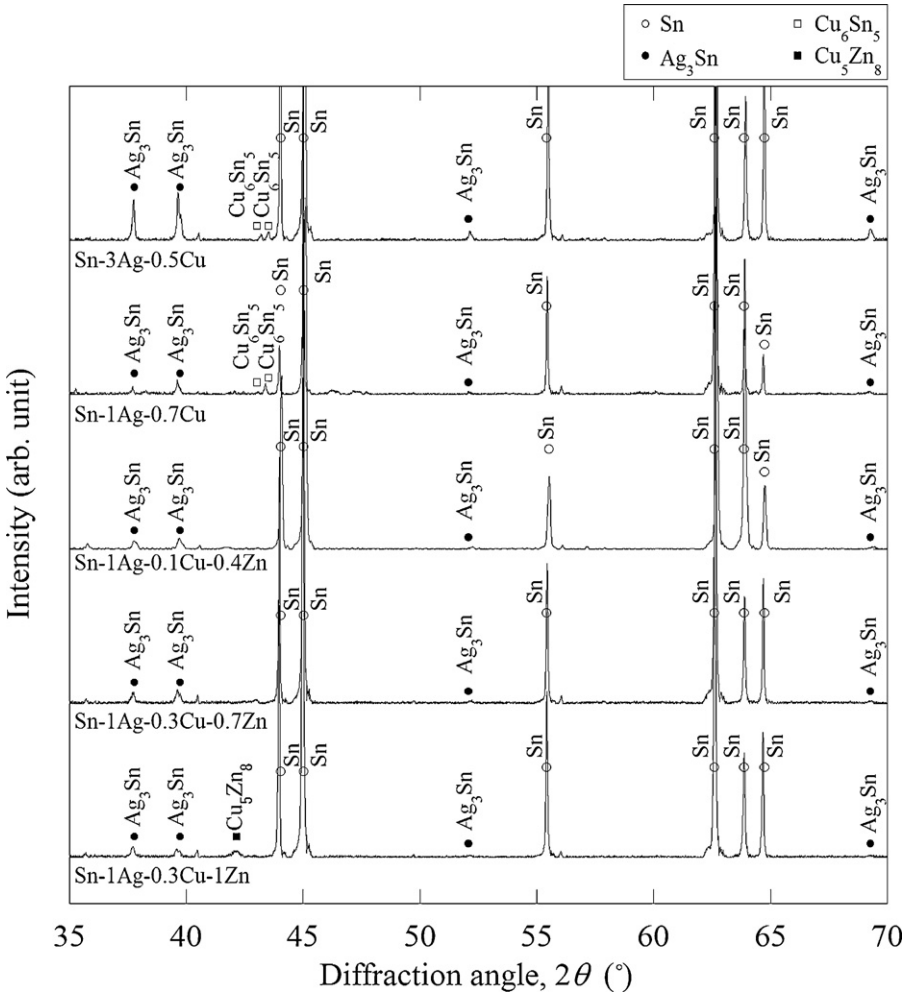

Fig. 3. X-ray diffraction patterns of Sn–Ag–Cu and Sn–Ag–Cu–Zn alloys before aging.

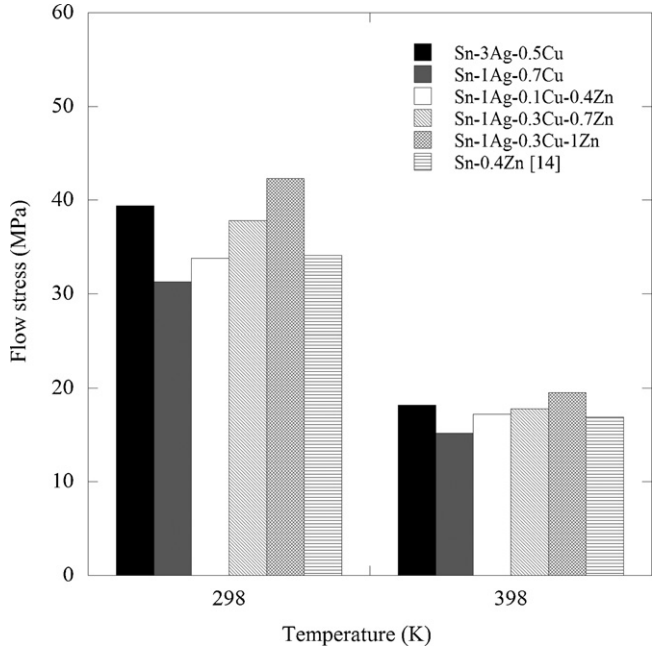

Fig. 4. Flow stress of Sn–Ag–Cu and Sn–Ag–Cu–Zn alloys at 298 K and 398 K before aging.

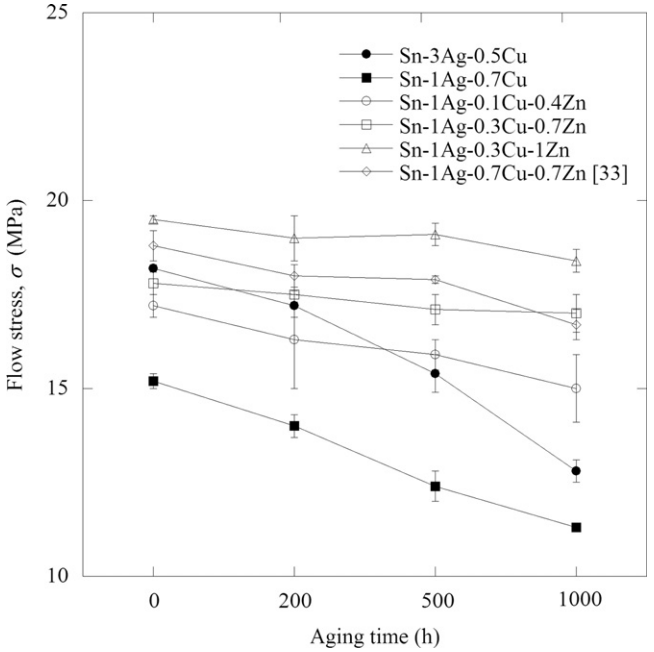

Fig. 5. Variation in flow stress as a function of aging time for the Sn–Ag–Cu and Sn–Ag–Cu–Zn alloys. Tensile tests were conducted at a temperature of 398 K and a strain rate of $1 \times 10^{-3}\ s^{-1}$.

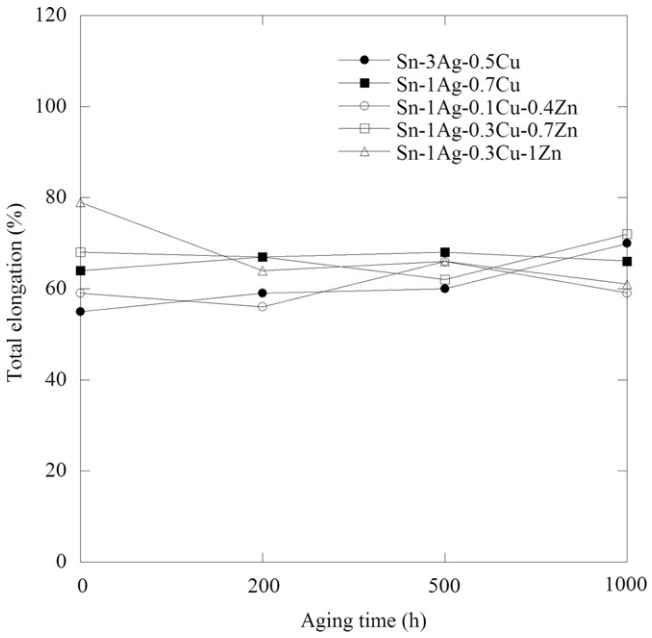

Fig. 6. Variation in total elongation as a function of aging time for Sn–Ag–Cu and Sn–Ag–Cu–Zn alloys. Tensile tests were conducted at a temperature of 398 K and a strain rate of 1×10^{-3} s^{-1}.

of dislocations. The dislocations bow out between the particles and subsequently bypass the particles, leaving a dislocation loop (Orowan loop) surrounding each particle. The bypassing stress is referred to as the Orowan stress. The Orowan stress before and after the aging treatment is also presented in Table 2. The addition of Zn to Sn–Ag–Cu inhibited the decrease in the Orowan stress after aging. Hence, the improvement in the thermal stability in terms of the flow stress with the addition of small amounts of Zn can be explained by the inhibition of the decrease in the Orowan stress. In dispersion hardening, finer particles obstruct the motion of dislocations more efficiently [46,49]. The coarsening of the intermetallic compound particles causes the decline in the flow stress after the aging treatment in Sn–3Ag–0.5Cu and Sn–1Ag–0.7Cu. For the Sn–Ag–Cu–Zn alloys, the Orowan stresses did not decrease much. The reason is probably that the addition of Zn to Sn–Ag–Cu alloys inhibited the growth of intermetallic compounds, as shown in Fig. 2.

The addition of small amounts of Zn to Sn–Ag–Cu increases the flow stress and improves the thermal stability in terms of the mechanical strength because of dispersion hardening and solid solution strengthening. Recently, many researchers have focused on finding a fourth element that will boost the mechanical strength of low-Ag Sn–Ag–Cu solders [21,22]. This study demonstrated that Zn is that element, despite the resulting poor wettability arising from its oxidation sensitivity, which is well known in Zn-rich solders such as Sn–9Zn [50,51]. However, the authors remain optimistic because the required amount of additional Zn in low-Ag Sn–Ag–Cu solders is very small; adding up to 1 wt.% of Zn is sufficient to improve the mechanical strength. In the future, the authors will present their findings on a low-Ag Sn–Ag–Cu–Zn solder for electronic component applications that demand highly reliable electrical interconnections.

5. Conclusions

In this study, we showed that the addition of small amounts of Zn to Sn–Ag–Cu increases the flow stress. The Sn–1Ag–0.3Cu–1Zn alloy exhibited higher flow stress than the Sn–3Ag–0.5Cu alloy. Dispersion hardening resulting from the presence of Ag_3Sn and Cu_5Zn_8 intermetallic compounds and solid solution strengthening due to solute Zn are the strengthening mechanisms in Sn–Ag–Cu–Zn alloys. Moreover, the addition of small amounts of Zn to Sn–Ag–Cu suppressed the decline in the flow stress after the aging treatment. After aging for 500 h at 398 K, the flow stresses of all Sn–Ag–Cu–Zn alloys (Sn–1Ag–0.1Cu–0.4Zn, Sn–1Ag–0.3Cu–0.7Zn, and Sn–1Ag–0.3Cu–1Zn) were higher than that of Sn–3Ag–0.5Cu. Because the addition of Zn to Sn–Ag–Cu alloys inhibited the growth of intermetallic compounds, the improvement in the thermal stability in terms of the flow stress after the addition of Zn can be explained by the inhibition of the decrease in the Orowan stress.

This study demonstrated that Zn is the sought-after fourth element that will boost the mechanical strength of low-Ag Sn–Ag–Cu solders. In the future, the authors will present their findings on a low-Ag Sn–Ag–Cu–Zn solder for electronic component applications that demand highly reliable electrical interconnections.

Acknowledgments

The authors thank Dr. T. Hirata at the Technology Research Institute of Osaka Prefecture for useful discussions and comments on the SEM observations. This research was partially supported by the Japan Science and Technology Agency (JST) Potentiality Verification Stage of Collaborative Development of Innovative Seeds program.

References

[1] G. Saad, A. Fawzy, E. Shawky, J. Alloys Compd. 479 (2009) 844–850.
[2] F. Cheng, F. Gao, H. Nishikawa, T. Takemoto, J. Alloys Compd. 472 (2009) 530–534.
[3] A.A. El-Daly, A.E. Hammad, J. Alloys Compd. 509 (2011) 8554–8560.
[4] A. Pietrikova, J. Bednarcik, J. Durisin, J. Alloys Compd. 509 (2011) 1550–1553.
[5] C.M. Miller, I.E. Anderson, J.F. Smith, J. Electron. Mater. 23 (1994) 595–601.
[6] X. Liu, M. Huang, Y. Zhao, C.M.L. Wu, L. Wang, J. Alloys Compd. 492 (2010) 433–438.
[7] J.W. Evans, A Guide to Lead-free Solders, first ed., Springer, London, 2007.
[8] K.S. Kim, S.H. Huh, K. Suganuma, J. Alloys Compd. 352 (2003) 226–236.
[9] Y.W. Yen, P.H. Tsai, Y.K. Fang, S.C. Lo, Y.P. Hsieh, C. Lee, J. Alloys Compd. 503 (2010) 25–30.
[10] F. Lin, W. Bi, G. Ju, W. Wang, X. Wei, J. Alloys Compd. 509 (2011) 6666–6672.
[11] H.R. Kotadia, O. Mokhtari, M.P. Clode, M.A. Green, S.H. Mannan, J. Alloys Compd. 511 (2012) 176–188.
[12] J.W. Yoon, B.I. Noh, S.B. Jung, J. Alloys Compd. 506 (2010) 331–337.
[13] L. Zhang, S.B. Xue, G. Zeng, L.L. Gao, H. Ye, J. Alloys Compd. 510 (2012) 38–45.
[14] J.W. Yoon, B.I. Noh, J.H. Yoon, H.B. Kang, S.B. Jung, J. Alloys Compd. 509 (2010) L153–L156.
[15] E. Hodulova, M. Palcut, E. Lechovic, B. Simekova, K. Ulrich, J. Alloys Compd. 509 (2011) 7052–7059.
[16] M. Shimoda, N. Hidaka, M. Yamashita, K. Sakaue, T. Ogawa, Proceedings of the 11th Electronic Packaging Technology Conference, 2009, pp. 725–730.
[17] N. Mookam, K. Kanlayasiri, J. Alloys Compd. 509 (2011) 6276–6279.
[18] M. Reid, J. Punch, M. Collins, C. Ryan, Solder. Surf. Mt. Technol. 20 (2008) 3–8.
[19] W. Liu, N.C. Lee, A. Porras, M. Ding, A. Gallagher, A. Huang, S. Chen, J.C. Lee, Proceedings of the 59th Electronic Components and Technology Conference (2009) 994–1007.
[20] C. Fangjie, G. Feng, Z. Jianyou, J. Wenshan, X. Xin, J. Mater. Sci. 46 (2011) 3424–3429.
[21] H.Y. Song, Q.S. Zhu, Z.G. Wang, J.K. Shang, M. Lu, Mater. Sci. Eng. 527 (2010) 1343–1350.
[22] S. Terashima, M. Tanaka, Mater. Trans. 45 (2004) 681–688.
[23] N. Hamada, M. Hamada, T. Uesugi, Y. Takigawa, K. Higashi, Mater. Trans. 51 (2010) 1747–1752.
[24] S.K. Kang, D.Y. Shih, D. Leonard, D.W. Henderson, T. Gosselin, S.I. Cho, J. Yu, W.K. Choi, JOM 56 (2004) 34–38.
[25] M. McCormack, G.W. Kammlott, H.S. Chen, S. Jin, Appl. Phys. Lett. 65 (1994) 1233–1235.
[26] A. Fawzy, Mater. Charact. 58 (2007) 323–331.
[27] S.K. Kang, D. Leonard, D.A.Y. Shih, L. Gignac, D.W. Henderson, S. Cho, J. Yu, J. Electron. Mater. 35 (2006) 479–485.
[28] F.J. Wang, F. Gao, X. Ma, Y.Y. Qian, J. Electron. Mater. 35 (2006) 1818–1824.
[29] M.G. Cho, S.K. Kang, D.Y. Shih, H.M. Lee, J. Electron. Mater. 36 (2007) 1501–1509.
[30] T.H. Chuang, H.J. Lin, J. Electron. Mater. 38 (2009) 420–424.
[31] Z.B. Luo, J. Zhao, Y.J. Gao, L. Wang, J. Alloys Compd. 500 (2010) 39–45.
[32] F.J. Wang, Z.S. Yu, K. Qi, J. Alloys Compd. 438 (2007) 110–115.
[33] R.L. Xu, Y.C. Liu, C. Wei, L.M. Yu, Solder. Surf. Mt. Technol. 22 (2010) 13–20.
[34] M. Lu, D.Y. Shih, S.K. Kang, C. Goldsmith, P. Flaitz, J. Appl. Phys. 106 (2009) 053509.

[35] H.R. Kotadia, O. Mokhtari, M. Bottrill, M.P. Clode, M.A. Green, S.H. Mannan, J. Electron. Mater. 39 (2010) 2720–2731.
[36] Y.K. Jee, Y.H. Ko, J. Yu, J. Mater. Res. 22 (2007) 1879–1887.
[37] H. Ma, J.C. Suhling, J. Mater. Sci. 44 (2009) 1141–1158.
[38] G. Li, Y. Shi, H. Hao, Z. Xia, Y. Lei, F. Guo, X. Li, J. Mater. Sci.: Mater. Electron. 20 (2009) 186–192.
[39] L. Snugovsky, C. Cermignani, D.D. Perovic, J.W. Rutter, J. Electron. Mater. 33 (2004) 1313–1315.
[40] K.W. Moon, W.J. Boettinger, U.R. Kattner, F.S. Biancaniello, C.A. Handwerker, J. Electron. Mater. 29 (2000) 1122–1136.
[41] C.E. Homer, H. Plummer, J. Inst. Met. 64 (1939) 169–200.
[42] N. Hamada, O. Takagi, K. Higashi, Y. Takigawa, T. Uesugi, WO/2009/051240, Ishikawa Metal Co., Ltd., Osaka Prefecture University Public Corporation, 2009.
[43] F. Ochoa, J.J. Williams, N. Chawla, JOM 55 (2003) 56–60.
[44] M. Kerr, N. Chawla, Acta Mater. 52 (2004) 4527–4535.
[45] T. Chen, I. Dutta, J. Electron. Mater. 37 (2008) 347–354.
[46] J.W. Martin, Precipitation Hardening, second ed., Butterworth-Heinemann, 1998.
[47] M. Fujiwara, T. Hirokawa, J. Jpn. Inst. Met. 51 (1987) 830–838.
[48] Z. Moser, J. Dutkiewicz, W. Gasior, J. Salawa, Bull. Alloy Phase Diagr. 6 (1985) 330–334.
[49] M. Mabuchi, K. Higashi, Acta Mater. 44 (1996) 4611–4618.
[50] X. Chen, A. Hu, M. Li, D. Mao, J. Alloys Compd. 460 (2008) 478–484.
[51] S. Vaynman, M.E. Fine, Scripta Mater. 41 (1999) 1269–1271.